Whightman function and scalar Casimir densities for a wedge with a cylindrical boundary

2005 J. Phys. A: Math. Gen. 38 8763

(http://iopscience.iop.org/0305-4470/38/40/017)

INSTITUTE OF PHYSICS PUBLISHING JOURNAL OF PHYSICS A: MATHEMATICAL AND GENERAL

J. Phys. A: Math. Gen. **38** (2005) 8763–8780 doi:10.1088/0305-4470/38/40/017

Whightman function and scalar Casimir densities for a wedge with a cylindrical boundary

A A Saharian and A S Tarloyan

Department of Physics, Yerevan State University, 1 Alex Manoogian St, 375049 Yerevan, Armenia

E-mail: saharyan@www.physdep.r.am

Received 7 April 2005, in final form 13 June 2005
Published 21 September 2005
Online at stacks.iop.org/JPhysA/38/8763

Abstract

The Whightman function, the vacuum expectation values of the field square and the energy–momentum tensor are investigated for a scalar field inside a wedge with and without a coaxial cylindrical boundary. Dirichlet boundary conditions are assumed on the bounding surfaces. The vacuum energy–momentum tensor is evaluated in the general case of the curvature coupling parameter. Making use of a variant of the generalized Abel-Plana formula, expectation values are presented as the sum of two terms. The first one corresponds to the geometry without a cylindrical boundary and the second one is induced by the presence of this boundary. The asymptotic behaviour of the field square, vacuum energy density and stresses near the boundaries are investigated. The additional vacuum forces acting on the wedge sides due the presence of the cylindrical boundary are evaluated and it is shown that these forces are attractive. As a limiting case, the geometry of two parallel plates perpendicularly intersected by a third one is analysed.

PACS numbers: 11.10.Kk, 03.70.+k

(Some figures in this article are in colour only in the electronic version)

1. Introduction

The influence of boundaries on the vacuum state of a quantum field leads to interesting physical consequences. The presence of reflecting boundaries alters the zero-point fluctuations spectrum and results in the shifts in the vacuum expectation values of quantities quadratic in the field, such as the energy density and stresses. In particular, vacuum forces arise acting on constraining boundaries. The particular features of these forces depend on the nature of the quantum field, the type of spacetime manifold, the boundary geometries and the specific boundary conditions imposed on the field. Since the original work by Casimir [1],

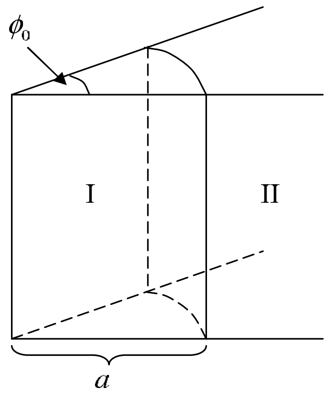

Figure 1. Geometry of a wedge with the opening angle ϕ_0 and cylindrical boundary of radius a.

many theoretical and experimental works have been done on this problem (see, e.g., [2–5] and references therein). However, there are still difficulties in both interpretation and renormalization of the Casimir effect. Moreover, the absence of a complete renormalization procedure, in practice, limits all exact calculations to the special case of highly symmetric boundary configurations (parallel plates, sphere, cylinder) with a specific background metric. From this point of view, the wedge with a cylindrical boundary is an interesting system, since the geometry is nontrivial and it includes two dynamical parameters, radius and angle, for phenomenological purposes. Due to the formal analogy that exists between a wedge and a straight cosmic string, the corresponding results can be applied to cosmic strings. In this paper, we will study the vacuum expectation values of the field square and the energy–momentum tensor for a massless scalar field with a general curvature coupling parameter inside a wedge of opening angle ϕ_0 with and without a coaxial cylindrical boundary assuming the Dirichlet boundary conditions on the constraining surfaces. Both regions inside and outside the cylindrical shell are considered. In the discussion below, we will call these regions region I and region II (see figure 1). Some most relevant investigations to the present paper are contained in [6–9] for a conformally coupled scalar and electromagnetic fields in a four-dimensional spacetime. The interaction between minimally and conformally coupled scalar fields and different boundary configurations constructed from parallel and orthogonal plane surfaces is studied in [10]. The total Casimir energy of a semi-circular infinite cylindrical shell with perfectly conducting walls is considered in [11] by using the zeta function technique. For a scalar field with an arbitrary curvature coupling parameter, the vacuum energy density in the geometry of a wedge with an arbitrary opening angle and with a cylindrical boundary is evaluated in [12]. This geometry is interesting from the point of view of general analysis for surface divergences in the expectation values of local physical observables for boundaries with discontinuities. The nonsmoothness of the boundary generates additional contributions to the heat kernel coefficients (see, for instance, the discussion in [13–15] and references therein). As in [12], our method here employs the mode summation and is based on a variant of the generalized Abel-Plana formula [16] combined with the point-splitting technique. This allows us to extract from the vacuum expectation values the parts due to a wedge without a cylindrical shell and to present the cylindrical parts in terms of strongly convergent integrals.

We have organized the paper as follows. The next section is devoted to the evaluation of the Whightman function for a massless scalar field with a general curvature coupling inside a wedge with a cylindrical boundary. By using the formula for the Whightman function, in section 3 we evaluate the vacuum expectation values of the field square and the energy–momentum tensor inside a wedge without a cylindrical boundary. In section 4, we consider the vacuum densities for a wedge with the cylindrical shell. Formulae for the shell contributions are derived and the corresponding surface divergences are investigated. The Whightman function, the vacuum expectation values of the field square and the energy–momentum tensor in the region II are considered in section 5. As a special case of the considered geometry, in section 6 we discuss the limiting case of two parallel plates perpendicularly intersected by the third plate. Finally, the results are summarized and discussed in section 7.

2. Whightman function inside a wedge

To describe the geometry of a wedge with the opening angle ϕ_0 and with the cylindrical boundary of radius a (see figure 1), we will use the cylindrical coordinates $(x^1, x^2, \ldots, x^D) = (r, \phi, z_1, \ldots, z_N)$, $N = D - 2$, where D is the number of spatial dimensions. Consider a massless scalar field φ with the curvature coupling parameter ξ, satisfying the field equation

$$(\nabla^i \nabla_i + \xi R)\varphi(x) = 0 \tag{2.1}$$

and obeying the Dirichlet boundary condition on the bounding surfaces:

$$\varphi|_{\phi=0} = \varphi|_{\phi=\phi_0} = \varphi|_{r=a} = 0. \tag{2.2}$$

We quote the generalization to other boundary conditions in section 7. In (2.1), ∇_i is the covariant derivative operator and R is the scalar curvature for the background spacetime. The values of the curvature coupling parameter $\xi = 0$ and $\xi = (D-1)/4D$ correspond to special cases of minimally and conformally coupled scalars, respectively. In this section, we evaluate the positive frequency Whightman function $\langle 0|\varphi(x)\varphi(x')|0\rangle$ in the region I, with $|0\rangle$ being the amplitude for the corresponding vacuum state. The response of a particle detector in an arbitrary state of motion is determined by this function (see, for instance, [17]). In addition, the vacuum expectation value of the energy–momentum tensor is expressed in terms of the Whightman function as

$$\langle 0|T_{ik}(x)|0\rangle = \lim_{x'\to x} \nabla_i \nabla'_k \langle 0|\varphi(x)\varphi(x')|0\rangle + \left[\left(\xi - \tfrac{1}{4}\right)g_{ik}\nabla^l\nabla_l - \xi\nabla_i\nabla_k\right]\langle 0|\varphi^2(x)|0\rangle. \tag{2.3}$$

Here we have assumed that the background spacetime is flat and have omitted the term with the Ricci tensor. By expanding the field operator and using the standard commutation relations, the Whightman function is presented as the mode sum

$$\langle 0|\varphi(x)\varphi(x')|0\rangle = \sum_\alpha \varphi_\alpha(x)\varphi^*_\alpha(x'), \tag{2.4}$$

where $\{\varphi_\alpha(x)\}$ is a complete orthonormal set of positive frequency solutions to the field equation, satisfying the corresponding boundary conditions, and α is a set of corresponding quantum numbers.

In the region $0 \leqslant r \leqslant a$ (region I in figure 1), the eigenfunctions satisfying the boundary conditions (2.2) on the wedge sides $\phi = 0, \phi_0$ have the form

$$\varphi_\alpha(x) = \beta_\alpha J_{qn}(\gamma r)\sin(qn\phi)\exp(\mathrm{i}\mathbf{k}\mathbf{r}_\parallel - \mathrm{i}\omega t), \qquad \alpha = (n, \gamma, \mathbf{k}), \tag{2.5}$$

$$\omega = \sqrt{\gamma^2 + k^2}, \qquad q = \pi/\phi_0, \qquad -\infty < k_j < \infty, \qquad n = 1, 2, \ldots, \tag{2.6}$$

where $\mathbf{k} = (k_1, \ldots, k_N)$, $\mathbf{r}_\parallel = (z_1, \ldots, z_N)$ and $J_l(z)$ is the Bessel function. The normalization coefficient β_α is determined from the standard Klein–Gordon scalar product with the integration over the region inside the wedge and is equal to

$$\beta_\alpha^2 = \frac{2}{(2\pi)^N \omega\phi_0 a^2 J'^2_{qn}(\gamma a)}. \tag{2.7}$$

The eigenvalues for the quantum number γ are quantized by the boundary condition (2.2) on the cylindrical surface $r = a$. From this condition, it follows that the possible values of γ are equal to

$$\gamma = \lambda_{n,j}/a, \qquad j = 1, 2, \ldots, \tag{2.8}$$

where $\lambda_{n,j}$ are the positive zeros of the Bessel function, $J_{qn}(\lambda_{n,j}) = 0$, arranged in ascending order, $\lambda_{n,j} < \lambda_{n,j+1}$. Substituting the eigenfunctions (2.5) into mode sum formula (2.4) with the set of quantum numbers $\alpha = (n, j, \mathbf{k})$, for the positive frequency Whightman function one finds

$$\langle 0|\varphi(x)\varphi(x')|0\rangle = \int \mathrm{d}^N\mathbf{k}\, \mathrm{e}^{\mathrm{i}\mathbf{k}(\mathbf{r}_\parallel - \mathbf{r}'_\parallel)} \sum_{n=1}^{\infty} \sin(qn\phi)\sin(qn\phi') \times \sum_{j=1}^{\infty} \beta_\alpha^2 J_{qn}(\gamma r) J_{qn}(\gamma r')\, \mathrm{e}^{-\mathrm{i}\omega(t-t')}|_{\gamma=\lambda_{n,j}/a}. \tag{2.9}$$

This formula is not convenient for the further evaluation of the vacuum expectation values of the field square and the energy–momentum tensor. This is related to that we do not know the explicit expressions for the eigenvalues $\lambda_{n,j}$ as functions on n and j, and the summands in the series over j are strongly oscillating functions for large values of j. In addition, the expression on the right-hand side of (2.9) is divergent in the coincidence limit and some renormalization procedure is needed to extract finite result for the vacuum expectation values of the field square and the energy–momentum tensor.

To obtain an alternative form for the Whightman function, we will apply to the sum over j a variant of the generalized Abel-Plana summation formula [16]

$$\sum_{j=1}^{\infty} \frac{2f(\lambda_{n,j})}{\lambda_{n,j} J_{qn}'^2(\lambda_{n,j})\sqrt{\lambda_{n,j}^2 + c^2}} = \int_0^{\infty} \frac{f(z)}{\sqrt{z^2+c^2}}\,\mathrm{d}z + \frac{\pi}{4}\mathrm{Res}_{z=0}\left[\frac{f(z)Y_{qn}(z)}{\sqrt{z^2+c^2}J_{qn}(z)}\right] - \frac{1}{\pi}\int_0^c \mathrm{d}z \frac{K_{qn}(z)}{I_{qn}(z)} \frac{\mathrm{e}^{-qn\pi\mathrm{i}} f(z\mathrm{e}^{\frac{\pi\mathrm{i}}{2}}) + \mathrm{e}^{qn\pi\mathrm{i}} f(z\mathrm{e}^{-\frac{\pi\mathrm{i}}{2}})}{\sqrt{c^2 - z^2}} + \frac{\mathrm{i}}{\pi}\int_c^{\infty} \mathrm{d}z \frac{K_{qn}(z)}{I_{qn}(z)} \frac{\mathrm{e}^{-qn\pi\mathrm{i}} f(z\mathrm{e}^{\frac{\pi\mathrm{i}}{2}}) - \mathrm{e}^{qn\pi\mathrm{i}} f(z\mathrm{e}^{-\frac{\pi\mathrm{i}}{2}})}{\sqrt{z^2 - c^2}}, \tag{2.10}$$

where $Y_l(z)$ is the Neumann function and $I_l(z)$, $K_l(z)$ are the Bessel modified functions. This formula is valid for functions $f(z)$ analytic in the right half-plane of the complex variable $z = x + \mathrm{i}y$ and satisfying the conditions

$$|f(z)| < \epsilon(x)\,\mathrm{e}^{c_1|y|}, \qquad c_1 < 2, \tag{2.11}$$

$$f(z) = o(z^{2qn-1}), \qquad z \to 0, \tag{2.12}$$

where $\epsilon(x) \to 0$ for $x \to \infty$. By taking in formula (2.10) $qn = 1/2$, as a particular case we receive the Abel-Plana formula (see, for instance, [2]). The generalized Abel-Plana formula was applied previously to a number of Casimir problems for spherically [18] and cylindrically [19, 20] symmetric boundaries and in the braneworld scenarios [21].

To evaluate the sum over j in (2.9) as a function $f(z)$, we choose

$$f(z) = zJ_{qn}(zr/a)J_{qn}(zr'/a)\exp\left[-\mathrm{i}\sqrt{k^2 + z^2/a^2}(t - t')\right]. \tag{2.13}$$

Using the asymptotic formulae of the Bessel functions for large values of arguments when n is fixed (see, e.g., [22]), we can see that for the function $f(z)$ from (2.13) the conditions (2.11) and (2.12) are satisfied if $r + r' + |t - t'| < 2a$. In particular, this is the case in the coincidence limit $t = t'$ for the region under consideration, $r, r' < a$. Formula (2.10) allows us to present the Whightman function in the form

$$\langle 0|\varphi(x)\varphi(x')|0\rangle = \langle 0_w|\varphi(x)\varphi(x')|0_w\rangle + \langle\varphi(x)\varphi(x')\rangle_a, \tag{2.14}$$

where

$$\langle 0_w|\varphi(x)\varphi(x')|0_w\rangle = \frac{1}{\phi_0}\int \frac{\mathrm{d}^N\mathbf{k}}{(2\pi)^N}\,\mathrm{e}^{\mathrm{i}\mathbf{k}(\mathbf{r}_\parallel-\mathbf{r}'_\parallel)}\int_0^\infty \mathrm{d}z\,\frac{z\,\mathrm{e}^{-\mathrm{i}(t-t')\sqrt{z^2+k^2}}}{\sqrt{z^2+k^2}} \times \sum_{n=1}^\infty \sin(qn\phi)\sin(qn\phi')J_{qn}(zr)J_{qn}(zr') \tag{2.15}$$

and

$$\langle\varphi(x)\varphi(x')\rangle_a = -\frac{2}{\pi\phi_0}\int \frac{\mathrm{d}^N\mathbf{k}}{(2\pi)^N}\,\mathrm{e}^{\mathrm{i}\mathbf{k}(\mathbf{r}_\parallel-\mathbf{r}'_\parallel)}\int_k^\infty \mathrm{d}z\,\frac{z\cosh[(t-t')\sqrt{z^2-k^2}]}{\sqrt{z^2-k^2}} \times \sum_{n=1}^\infty \sin(qn\phi)\sin(qn\phi')I_{qn}(zr)I_{qn}(zr')\frac{K_{qn}(za)}{I_{qn}(za)}. \tag{2.16}$$

In the limit $a \to \infty$ for fixed r, r', the term $\langle\varphi(x)\varphi(x')\rangle_a$ vanishes and, hence, the term $\langle 0_w|\varphi(x)\varphi(x')|0_w\rangle$ is the Whightman function for the wedge without a cylindrical boundary with the corresponding vacuum state $|0_w\rangle$. Consequently, the term $\langle\varphi(x)\varphi(x')\rangle_a$ is induced by the presence of the cylindrical boundary. Hence, the application of the generalized Abel-Plana formula allowed us to extract from the Whightman function the part due to the wedge without a cylindrical boundary. For the points away from the cylindrical surface, the additional part induced by this surface, formula (2.16), is finite in the coincidence limit and the renormalization is needed only for the part coming from the term (2.15).

3. Vacuum expectation values inside a wedge without a cylindrical boundary

In this section, we consider the geometry of a wedge without a cylindrical boundary. Expression (2.15) for the corresponding Whightman function can be simplified by using the formula [23]

$$\sum_{n=0}^{\infty}{}' \cos nb J_{qn}(u)J_{qn}(v) = \frac{1}{2q}\sum_{n=n_-}^{n_+}\alpha_n J_0\left(\sqrt{u^2+v^2-2uv\cos\frac{2\pi n+b}{q}}\right), \tag{3.1}$$

where $n_\pm = \pm[(q\pi \mp b)/(2\pi)]$ (square brackets mean the integer value of the enclosed expression), $\alpha_n = 1$ for $n \neq n_\pm$, $\alpha_{n_\pm} = 1/2$ for $|(q\pi \mp b)/(2\pi)| = 0, 1, 2, \ldots$, $\alpha_{n_\pm} = 1$ for $|(q\pi \mp b)/(2\pi)| \neq 0, 1, 2, \ldots$ and the prime means that the summand with $n = 0$ should be taken with the weight 1/2. This formula is valid for integer values of $q = \pi/\phi_0 \geqslant 1$. The results for other values q are obtained from the formulae for the renormalized vacuum expectation values derived below in this section by analytic continuation over ϕ_0. Making use of formula (3.1), for the sum over n in formula (2.15) one finds

$$\sum_{n=1}^\infty \sin(qn\phi)\sin(qn\phi')J_{qn}(zr)J_{qn}(zr') = \frac{1}{4q}\sum_{j=1}^{2}(-1)^{j+1}\sum_{n=n_{j-}}^{n_{j+}}\alpha_n J_0(zu_j), \tag{3.2}$$

where

$$u_j = \sqrt{r^2+r'^2-2rr'\cos[2n\phi_0+\phi+(-1)^j\phi']}, \tag{3.3}$$

$$n_{j\pm} = \pm\left[\frac{\pi \mp (\phi+(-1)^j\phi')}{2\phi_0}\right]. \tag{3.4}$$

Now, evaluating the integral over z in (2.15) with the help of the formula [23]

$$\int_0^\infty \mathrm{d}z \frac{z\,\mathrm{e}^{-\mathrm{i}(t-t')\sqrt{z^2+k^2}}}{\sqrt{z^2+k^2}} J_0(zu_j) = \frac{\mathrm{e}^{-k\sqrt{u_j^2-(t-t')^2}}}{\sqrt{u_j^2-(t-t')^2}}, \tag{3.5}$$

the expression of the Whightman function is presented in the form

$$\langle 0_w|\varphi(x)\varphi(x')|0_w\rangle = \sum_{j=1}^{2} \frac{(-1)^{j+1}}{2(2\pi)^{N+1}} \sum_{n=n_{j-}}^{n_{j+}} \alpha_n \int \mathrm{d}^N\mathbf{k}\,\mathrm{e}^{\mathrm{i}\mathbf{k}(\mathbf{r}_\parallel-\mathbf{r}'_\parallel)} \frac{\mathrm{e}^{-k\sqrt{u_j^2-(t-t')^2}}}{\sqrt{u_j^2-(t-t')^2}}. \tag{3.6}$$

For the integral in this formula, one has

$$\int \mathrm{d}^N\mathbf{k}\,\mathrm{e}^{\mathrm{i}\mathbf{k}(\mathbf{r}_\parallel-\mathbf{r}'_\parallel)} \frac{\mathrm{e}^{-k\sqrt{u_j^2-(t-t')^2}}}{\sqrt{u_j^2-(t-t')^2}} = \frac{2^N\pi^{(N-1)/2}\Gamma\left(\frac{N+1}{2}\right)}{\left[u_j^2+|\mathbf{r}_\parallel-\mathbf{r}'_\parallel|^2-(t-t')^2\right]^{(N+1)/2}}, \tag{3.7}$$

with $\Gamma(z)$ being the Euler gamma function. Hence, for the Whightman function in the geometry of a wedge without a cylindrical boundary, one obtains the formula

$$\langle 0_w|\varphi(x)\varphi(x')|0_w\rangle = \frac{\Gamma\left(\frac{D-1}{2}\right)}{4\pi^{\frac{D+1}{2}}} \sum_{j=1}^{2} \sum_{n=n_{j-}}^{n_{j+}} \frac{(-1)^{j+1}\alpha_n}{\left[u_j^2+|\mathbf{r}_\parallel-\mathbf{r}'_\parallel|^2-(t-t')^2\right]^{(D-1)/2}}. \tag{3.8}$$

Note that for the Whightman function of the Minkowski space without boundaries, one has

$$\langle 0_M|\varphi(x)\varphi(x')|0_M\rangle = \frac{\Gamma\left(\frac{D-1}{2}\right)}{4\pi^{\frac{D+1}{2}}[|\mathbf{r}-\mathbf{r}'|^2-(t-t')^2]^{(D-1)/2}}, \tag{3.9}$$

where $|0_M\rangle$ is the amplitude for the vacuum state in the Minkowski spacetime without boundaries. This function coincides with the $j = 1, n = 0$ term in formula (3.8). Taking the coincidence limit $x' \to x$, for the difference of the vacuum expectation values of the field square,

$$\langle\varphi^2(x)\rangle_{\mathrm{ren}}^{(w)} = \langle 0_w|\varphi^2(x)|0_w\rangle - \langle 0_M|\varphi^2(x)|0_M\rangle, \tag{3.10}$$

we find

$$\langle\varphi^2(x)\rangle_{\mathrm{ren}}^{(w)} = \frac{\Gamma\left(\frac{D-1}{2}\right)}{(4\pi)^{\frac{D+1}{2}}r^{D-1}} {\sum_{j=1}^{2}}' \sum_{n=\bar{n}_{j-}}^{\bar{n}_{j+}} \frac{(-1)^{j+1}\alpha_n}{|\sin\phi_n^{(j)}|^{D-1}}, \tag{3.11}$$

where the prime means that the term $j = 1, n = 0$ has to be omitted, and we use the notations

$$\phi_n^{(j)} = n\phi_0 + \phi\frac{1+(-1)^j}{2}, \tag{3.12}$$

$$\bar{n}_{j\pm} = \pm\left[\frac{\pi \mp \phi(1+(-1)^j)}{2\phi_0}\right]. \tag{3.13}$$

In equation (3.11), $\alpha_n = 1$ for $n \neq \bar{n}_{j\pm}$, $\alpha_{\bar{n}_{j\pm}} = 1/2$ for $|\pi \mp \phi(1+(-1)^j)|/2\phi_0 = 0, 1, 2, \ldots$ and $\alpha_{\bar{n}_{j\pm}} = 1$ for $|\pi \mp \phi(1+(-1)^j)|/2\phi_0 \neq 0, 1, 2, \ldots$. In the case $D = 3$, by using the formula

$$\sum_{n=0}^{m-1} \sec^2\left(x + \frac{n\pi}{m}\right) = m^2\csc^2\left(mx + \frac{m\pi}{2}\right), \tag{3.14}$$

for the renormalized vacuum expectation value of the field square one finds [7]

$$\langle\varphi^2(x)\rangle_{\mathrm{ren}}^{(w)} = \frac{q^2-1-3q^2\csc^2(q\phi)}{48\pi^2r^2}. \tag{3.15}$$

Near the wedge boundaries $\phi = \phi_m$, $m = 0, 1$ ($\phi_1 = 0$), the main contribution in (3.11) comes from the terms $j = 2$, $n = 0$ and $n = -1$ for $m = 0$ and $m = 1$, respectively, and the renormalized vacuum expectation value of the field square diverges with the leading behaviour

$$\langle\varphi^2(x)\rangle_{\rm ren}^{(w)} = -\frac{\Gamma\left(\frac{D-1}{2}\right)}{(4\pi)^{\frac{D+1}{2}}(r|\phi-\phi_m|)^{D-1}}, \qquad \phi \to \phi_m. \tag{3.16}$$

The surface divergences in renormalized vacuum expectation values of the local physical observables are well known in quantum field theory with boundaries and result from the idealization of the boundaries as perfectly smooth surfaces which are perfect reflectors at all frequencies. These divergences are investigated in detail for various types of fields and general shape of smooth boundary [7, 24]. Near the smooth boundary, the leading divergence in the field square varies as $(D-1)$th power of the distance from the boundary. It seems plausible that such effects as surface roughness, or the microstructure of the boundary on small scales (the atomic nature of matter for the case of the electromagnetic field [25]), can introduce a physical cut-off needed to produce finite values of surface quantities. An alternative mechanism for introducing a cut-off which removes singular behaviour on boundaries is to allow the position of the boundary to undergo quantum fluctuations [26]. Such fluctuations smear out the contribution of the high frequency modes without the need to introduce an explicit high frequency cut-off.

Now we turn to the vacuum expectation values of the energy–momentum tensor. By making use of formula (2.3), for the non-zero components one obtains (no summation over i)

$$\langle T_i^i\rangle_{\rm ren}^{(w)} = -\frac{\Gamma\left(\frac{D+1}{2}\right)}{2^{D+2}\pi^{\frac{D+1}{2}}r^{D+1}}\sum_{j=1}^{2}{}'\sum_{n=\bar{n}_{j-}}^{\bar{n}_{j+}}\frac{(-1)^{j+1}\alpha_n f_{jn}^{(i)}}{\left|\sin\phi_n^{(j)}\right|^{D+1}}, \tag{3.17}$$

$$\langle T_2^1\rangle_{\rm ren}^{(w)} = -\frac{D(\xi-\xi_c)\Gamma\left(\frac{D+1}{2}\right)}{2^D\pi^{\frac{D+1}{2}}r^D}\sum_{n=\bar{n}_{2-}}^{\bar{n}_{2+}}\frac{\alpha_n\sin\phi_n^{(2)}\cos\phi_n^{(2)}}{\left|\sin\phi_n^{(2)}\right|^{D+1}}, \tag{3.18}$$

where $i = 0, 1, \ldots, D$, and we use the following notations:

$$f_{jn}^{(i)} = 1 + (4\xi - 1)\left[(D-1)\delta_{j1}\sin^2\phi_n^{(j)} + D\delta_{j2}\right], \qquad i = 0, 3, \ldots, D, \tag{3.19}$$

$$f_{jn}^{(1)} = f_{jn}^{(0)} - 4D(\xi-\xi_c)\sin^2\phi_n^{(j)}, \tag{3.20}$$

$$f_{jn}^{(2)} = D\left[4\sin^2\phi_n^{(j)}(\xi - \xi_c\delta_{j2}) - \delta_{j1}\right]. \tag{3.21}$$

In the case $\phi_0 = \pi/2$ and for minimally and conformally coupled scalar fields, it can be checked that from formulae (3.17) and (3.18), after the transformation from cylindrical coordinates to the Cartesian ones, as a special case we obtain the result derived in [10]. For a scalar field with a general curvature coupling parameter, the vacuum energy–momentum tensor is non-diagonal. For the conformally coupled scalar field, this tensor is diagonal and does not depend on the angular coordinate ϕ. From the continuity equation $\nabla_k T_i^k = 0$ for the energy–momentum tensor, one has the following relations for the components:

$$\partial_r\left(rT_2^1\right) + r\partial_\phi T_2^2 = 0, \tag{3.22}$$

$$\partial_r\left(rT_1^1\right) + r\partial_\phi T_1^2 = T_2^2. \tag{3.23}$$

In the case of a conformally coupled scalar field, we have an additional zero trace condition. It can be checked that vacuum expectation values (3.17) and (3.18) satisfy equations (3.22) and (3.23).

For a non-conformally coupled field, vacuum expectation values (3.17) diverge on the boundaries $\phi = \phi_m$. For the points near these boundaries, the leading terms in the corresponding asymptotic expansions are given by relations (no summation over $i, i = 0, 3, \ldots, D$)

$$\langle T_i^i \rangle_{\text{ren}}^{(w)} \approx \frac{\langle T_2^2 \rangle_{\text{ren}}^{(w)}}{(\phi - \phi_m)^2} \approx \frac{-\langle T_2^1 \rangle_{\text{ren}}^{(w)}}{r(\phi - \phi_m)} \approx \frac{D(\xi - \xi_c)\Gamma\left(\frac{D+1}{2}\right)}{2^D \pi^{\frac{D+1}{2}} (r|\phi - \phi_m|)^{D+1}}. \tag{3.24}$$

For the points away from the edge $r = 0$, this leading behaviour is the same as that for the geometry of a single plate.

In the most important case $D = 3$, by using formula (3.14), for the components of the renormalized energy–momentum tensor we find

$$\langle T_0^0 \rangle_{\text{ren}}^{(w)} = \langle T_3^3 \rangle_{\text{ren}}^{(w)} = \frac{1}{32\pi^2 r^4} \left\{ \frac{1 - q^4}{45} + \frac{8}{3}(1 - q^2)(\xi - \xi_c) \right.$$
$$\left. + 12 \frac{(\xi - \xi_c) q^2}{\sin^2(q\phi)} \left[\frac{q^2}{\sin^2(q\phi)} - \frac{2}{3} q^2 + \frac{2}{3} \right] \right\}, \tag{3.25}$$

$$\langle T_1^1 \rangle_{\text{ren}}^{(w)} = \frac{1}{32\pi^2 r^4} \left\{ \frac{1 - q^4}{45} - \frac{4}{3}(1 - q^2)(\xi - \xi_c) + 12 \frac{(\xi - \xi_c) q^2}{\sin^2(q\phi)} \left[\frac{q^2}{\sin^2(q\phi)} - \frac{2}{3} q^2 - \frac{1}{3} \right] \right\}, \tag{3.26}$$

$$\langle T_2^1 \rangle_{\text{ren}}^{(w)} = -\frac{3(\xi - \xi_c)}{8\pi^2 r^3} \frac{q^3 \cos(q\phi)}{\sin^3(q\phi)}, \tag{3.27}$$

$$\langle T_2^2 \rangle_{\text{ren}}^{(w)} = \frac{1}{8\pi^2 r^4} \left[\frac{q^4 - 1}{60} + (\xi - \xi_c) \left(1 - q^2 + \frac{3q^2}{\sin^2(q\phi)} \right) \right]. \tag{3.28}$$

For a conformally coupled scalar field, this tensor coincides with the result previously obtained in the literature [6, 7]. The corresponding vacuum forces acting on the wedge sides are determined by the effective pressure $-\langle T_2^2 \rangle_{\text{ren}}^{(w)}$. These forces are attractive for the wedge with $q > 1$ and are repulsive for $q < 1$. Formula (3.25) for the component $\langle T_0^0 \rangle_{\text{ren}}^{(w)}$ is derived in [12] by a different way. For the electromagnetic field in $D = 3$, the vacuum expectation values of the energy–momentum tensor are considered in [7, 8] for a perfectly conducting wedge and in [9] for a dielectric wedge. In both cases, the vacuum energy–momentum tensor is uniform. This is a consequence of the conformal invariance of the electromagnetic field.

4. Field square and the vacuum energy–momentum tensor in the region I

We now turn to the geometry of a wedge with additional cylindrical boundary of radius a. Taking the coincidence limit $x' \to x$ in formula (2.14) for the Whightman function and integrating over $\mathbf{k}$ with the help of the formula [20]

$$\int d^N \mathbf{k} \int_k^\infty \frac{k^s g(z)\, dz}{\sqrt{z^2 - k^2}} = \frac{\pi^{N/2}}{\Gamma(N/2)} B\left(\frac{N+s}{2}, \frac{1}{2} \right) \int_0^\infty dz\, z^{N+s-1} g(z), \tag{4.1}$$

where $B(x, y)$ is the Euler beta function, the vacuum expectation value of the field square is presented as a sum of two terms

$$\langle 0|\varphi^2|0\rangle = \langle 0_w|\varphi^2|0_w\rangle + \langle \varphi^2 \rangle_a, \tag{4.2}$$

where the part induced by the cylindrical boundary is given by the formula

$$\langle\varphi^2\rangle_a = -\frac{2^{3-D}\pi^{\frac{1-D}{2}}}{\Gamma\left(\frac{D-1}{2}\right)a^{D-1}\phi_0}\sum_{n=1}^{\infty}\sin^2(qn\phi)\int_0^\infty \mathrm{d}z\, z^{D-2}\frac{K_{qn}(z)}{I_{qn}(z)}I_{qn}^2(zr/a). \tag{4.3}$$

Note that this part vanishes at the wedge sides $\phi = \phi_m$, $0 \leqslant r < a$. Near the edge $r = 0$, the main contribution into $\langle\varphi^2\rangle_a$ comes from the summand $n = 1$ and one has

$$\langle\varphi^2\rangle_a \approx \frac{4\Gamma^{-2}(q+1)\sin^2(q\phi)\mathcal{F}_D(q)}{(4\pi)^{\frac{D-1}{2}}\Gamma\left(\frac{D-1}{2}\right)a^{D-1}\phi_0}\left(\frac{r}{2a}\right)^{2q} \tag{4.4}$$

for $r \ll a$, with the notation

$$\mathcal{F}_D(q) = \int_0^\infty \mathrm{d}z\, z^{D+2q-2}\frac{K_q(z)}{I_q(z)}. \tag{4.5}$$

The part $\langle\varphi^2\rangle_a$ diverges on the cylindrical surface $r = a$. Near this surface, the main contribution into (4.3) comes from large values n. Introducing a new integration variable $z \to nqz$, replacing the Bessel modified functions by their uniform asymptotic expansions for large values of the order (see, for instance, [22]) and expanding over $a - r$, for $|\phi - \phi_m| \gg 1 - r/a$ to the leading order one finds

$$\begin{aligned}\langle\varphi^2\rangle_a &\approx -\frac{(q/2a)^{D-1}}{\pi^{\frac{D+1}{2}}\Gamma\left(\frac{D-1}{2}\right)}\int_0^\infty \mathrm{d}z\frac{z^{D-1}}{\sqrt{1+z^2}}\sum_{n=1}^{\infty}n^{D-2}\,\mathrm{e}^{-2nq(1-r/a)\sqrt{1+z^2}}\\ &\approx -\frac{\Gamma\left(\frac{D-1}{2}\right)}{(4\pi)^{\frac{D+1}{2}}(a-r)^{D-1}}.\end{aligned} \tag{4.6}$$

This leading behaviour is the same as that for a cylindrical surface of radius a.

Similarly, the vacuum expectation value of the energy–momentum tensor for the situation when the cylindrical boundary is present is written in the form

$$\langle 0|T_{ik}|0\rangle = \langle 0_w|T_{ik}|0_w\rangle + \langle T_{ik}\rangle_a, \tag{4.7}$$

where $\langle T_{ik}\rangle_a$ is induced by the cylindrical boundary. This term is obtained from the corresponding part in the Whightman function, $\langle\varphi(x)\varphi(x')\rangle_a$, acting by the appropriate differential operator and taking the coincidence limit (see formula (2.3)). For the points away from the cylindrical surface, this limit gives a finite result. For the corresponding components of the energy–momentum tensor, one obtains (no summation over i)

$$\begin{aligned}\langle T_i^i\rangle_a = {}& \frac{(4\pi)^{-\frac{D-1}{2}}}{\Gamma\left(\frac{D-1}{2}\right)a^{D+1}\phi_0}\sum_{n=1}^{\infty}\int_0^\infty \mathrm{d}z\, z^D\frac{K_{qn}(z)}{I_{qn}(z)}\\ &\times\left\{a_{i,qn}^{(+)}[I_{qn}(y)] - a_{i,qn}^{(-)}[I_{qn}(y)]\cos(2qn\phi)\right\}, \qquad y = \frac{zr}{a},\end{aligned} \tag{4.8}$$

$$\begin{aligned}\langle T_2^1\rangle_a = {}& \frac{2(4\pi)^{-\frac{D-1}{2}}}{\Gamma\left(\frac{D-1}{2}\right)a^D\phi_0}\sum_{n=1}^{\infty}qn\sin(2qn\phi)\int_0^\infty \mathrm{d}z\, z^{D-1}\frac{K_{qn}(z)}{I_{qn}(z)}\\ &\times I_{qn}(y)\left[\frac{2\xi}{y}I_{qn}(y) + (1-4\xi)I'_{qn}(y)\right],\end{aligned} \tag{4.9}$$

with the notations

$$a_{i,l}^{(\pm)}[g(y)] = (4\xi - 1)\left\{g'^2(y) + g^2(y)\left[1 \pm \frac{l^2}{y^2} + \frac{2}{(D-1)(4\xi-1)}\right]\right\}, \tag{4.10}$$

$$a_{1,l}^{(\pm)}[g(y)] = g'^2(y) + \frac{4\xi}{y}g(y)g'(y) - g^2(y)\left\{1 \pm [1-4\xi(1\mp 1)]\frac{l^2}{y^2}\right\}, \tag{4.11}$$

$$a_{2,l}^{(\pm)}[g(y)] = (4\xi-1)[g'^2(y)+g^2(y)] - \frac{4\xi}{y}g(y)g'(y) + \frac{l^2}{y^2}g^2(y)(4\xi\pm 1), \tag{4.12}$$

for a given function $g(y)$, $i = 0, 3, \ldots, D$. Formula (4.8) for the energy density ($i = 0$) was previously derived in [12]. In accordance with the problem symmetry, the expressions for the diagonal components are invariant under the replacement $\phi \to \phi_0 - \phi$ and the off-diagonal component $\langle T_2^1\rangle_a$ changes the sign under this replacement. Note that the latter vanishes on the wedge sides $\phi = \phi_m, 0 \leqslant r < a$ and for $\phi = \phi_0/2$. On the wedge sides one has $\cos(2qn\phi) = 1$ and for the diagonal components of the energy–momentum tensor we obtain (no summation over i)

$$\langle T_i^i\rangle_a\big|_{\phi=\phi_m} = \frac{2^{2-D}\pi^{\frac{5-D}{2}}A_i}{\Gamma\left(\frac{D-1}{2}\right)a^{D-1}r^2\phi_0^3}\sum_{n=1}^{\infty}n^2\int_0^{\infty}\mathrm{d}z\, z^{D-2}\frac{K_{qn}(z)}{I_{qn}(z)}I_{qn}^2(zr/a), \tag{4.13}$$

where $A_i = 4\xi - 1, i = 0, 1, 3, \ldots, D, A_2 = 1$. In particular, the additional vacuum effective pressure in the direction perpendicular to the wedge sides, $p_a = -\langle T_2^2\rangle_a\big|_{\phi=\phi_m}$, does not depend on the curvature coupling parameter and is negative for all values $0 < r < a$. This means that the vacuum forces acting on the wedge sides $\phi = \phi_m$ due to the presence of the cylindrical boundary are attractive. The corresponding vacuum stresses in the directions parallel to the wedge sides are isotropic and the energy density is negative for both minimally and conformally coupled scalars. It can be checked that expectation values (4.8) and (4.9) satisfy equations (3.22) and (3.23) and, hence, the continuity equation for the energy–momentum tensor. Aiming to compare with the result for the energy–momentum tensor of a cylindrical shell with the radius a, let us write down the corresponding formula, which is obtained from the general result of [20] and has the form

$$\langle T_i^k\rangle_{\mathrm{ren}}^{\mathrm{cyl}} = \frac{2(4\pi)^{-\frac{D+1}{2}}\delta_i^k}{a^{D+1}\Gamma\left(\frac{D-1}{2}\right)}\sum_{n=-\infty}^{+\infty}\int_0^{\infty}\mathrm{d}z\, z^D\frac{K_n(z)}{I_n(z)}a_{i,n}^{(+)}[I_n(zr/a)], \tag{4.14}$$

with the same notations as in (4.10)–(4.12).

For $0 < r < a$, the cylindrical parts (4.8) and (4.9) are finite for all values $0 \leqslant \phi \leqslant \phi_0$, including the wedge sides. The divergences on these sides are included in the first term on the right-hand side of (4.7) corresponding to the case without cylindrical boundary. Near the edge $r = 0$, the main contribution into the boundary part (4.8) comes from the summand with $n = 1$ and one has

$$\langle T_i^i\rangle_a \approx \frac{q\left[B_i^{(+)} - B_i^{(-)}\cos(2q\phi)\right]\mathcal{F}_D(q)}{(4\pi)^{\frac{D+1}{2}}a^{D+1}\Gamma\left(\frac{D-1}{2}\right)\Gamma^2(q)}\left(\frac{r}{2a}\right)^{2q-2}, \tag{4.15}$$

$$\langle T_2^1\rangle_a \approx \frac{[2\xi + (1-4\xi)q]\sin(2q\phi)\mathcal{F}_D(q)}{\pi(4\pi)^{\frac{D-1}{2}}a^D\Gamma\left(\frac{D-1}{2}\right)\Gamma^2(q)}\left(\frac{r}{2a}\right)^{2q-1}, \tag{4.16}$$

with the notations

$$B_i^{(\pm)} = (4\xi-1)(1\pm 1), \qquad i = 0, 3, \ldots, D,$$
$$B_1^{(\pm)} = 4\xi(1/q - 1 \pm 1) \mp 1 + 1, \qquad B_2^{(\pm)} = 4\xi(2-1/q) \pm 1 - 1, \tag{4.17}$$

and the function $\mathcal{F}_D(q)$ is defined by formula (4.5).

The boundary part $\langle T_i^k\rangle_a$ diverges on the cylindrical surface $r = a$. Introducing a new integration variable $z \to nqz$ and by taking into account that near the surface $r = a$ the main contribution comes from the large values of n, we can replace the Bessel modified functions by their uniform asymptotic expansions for large values of the order. Expanding over $a-r$, to the leading order for the diagonal components one finds

$$\langle T_i^i\rangle_a \approx \frac{(4\pi)^{-\frac{D-1}{2}}}{2\Gamma\left(\frac{D-1}{2}\right)a^{D+1}\phi_0}\sum_{n=1}^{\infty}(qn)^D\int_0^{\infty}\mathrm{d}z\, z^{D-2}(1+z^2)^{1/2} \times \mathrm{e}^{-2nq(1-r/a)\sqrt{1+z^2}}\left[A_i^{(+)}(z)-A_i^{(-)}(z)\cos(2qn\phi)\right], \tag{4.18}$$

where

$$A_0^{(\pm)}(y)=(4\xi-1)\left\{1+\frac{1}{1+y^2}\left[y^2\pm 1+\frac{2y^2}{(D-1)(4\xi-1)}\right]\right\}, \tag{4.19}$$

$$A_1^{(\pm)}(y)=1-\frac{1}{1+y^2}[y^2\pm 1+4\xi(1\mp 1)], \tag{4.20}$$

$$A_2^{(\pm)}(y)=4\xi-1+\frac{1}{1+y^2}[y^2(4\xi-1)+4\xi\pm 1]. \tag{4.21}$$

On the wedge sides, one has $\cos(2qn\phi)=1$ and this yields

$$\langle T_i^i\rangle_a\big|_{\phi=\phi_m} \approx \frac{(4\pi)^{-\frac{D-1}{2}}A_i}{\Gamma\left(\frac{D-1}{2}\right)a^{D+1}\phi_0}\sum_{n=1}^{\infty}(qn)^D\int_0^{\infty}\frac{\mathrm{d}z\, z^{D-2}}{\sqrt{1+z^2}}\mathrm{e}^{-2nq(1-r/a)\sqrt{1+z^2}}, \tag{4.22}$$

where the coefficients A_i are defined in the paragraph after formula (4.13). Summing over n, to the leading order over $(a-r)^{-1}$ one finds

$$\langle T_i^i\rangle_a\big|_{\phi=\phi_m} \approx \frac{A_i\Gamma\left(\frac{D+1}{2}\right)}{2(4\pi)^{\frac{D+1}{2}}(a-r)^{D+1}}, \qquad r\to a. \tag{4.23}$$

It can be seen that for the non-diagonal component to the leading order one has $\langle T_2^1\rangle_a \sim (a-r)^{-D}$.

For the angles $0<\phi<\phi_0$, by using the formula

$$\sum_{n=1}^{\infty} n^D \mathrm{e}^{-\alpha n}\cos n\beta = \frac{(-1)^D}{2}\frac{\mathrm{d}^D}{\mathrm{d}\alpha^D}\left(\frac{\sinh\alpha}{\cosh\alpha-\cos\beta}-1\right), \tag{4.24}$$

introducing a new integration variable $y=2\pi(1-r/a)\sqrt{1+z^2}/\phi_0$ and expanding over $(1-r/a)$, one finds that for $|\phi-\phi_m|\gg 1-r/a$ the leading contribution of the term with $A_i^{(+)}(z)$ dominates and to the leading order we find

$$\langle T_i^i\rangle_a \approx \frac{D(\xi-\xi_c)\Gamma\left(\frac{D+1}{2}\right)}{2^D\pi^{(D+1)/2}(a-r)^{D+1}}, \qquad i=0,2,\ldots,D. \tag{4.25}$$

This leading divergence coincides with the corresponding one for a cylindrical surface of the radius a (see, for instance, [20]). For the other components to the leading order one has $\langle T_1^1\rangle_a \sim \langle T_2^1\rangle_a \sim (a-r)^{-D}$. In figures 2 and 3, we have plotted the dependences of the boundary-induced vacuum expectation values for the components of the energy–momentum tensor in the case of $D=3$ conformally coupled scalar field as functions on coordinates $x=(r/a)\cos\phi$, $y=(r/a)\sin\phi$ for a wedge with $\phi_0=\pi/2$. In particular, the corresponding energy density is negative everywhere and the vacuum forces determined by the component $\langle T_2^2\rangle_a\big|_{\phi=\phi_m}$ are attractive.

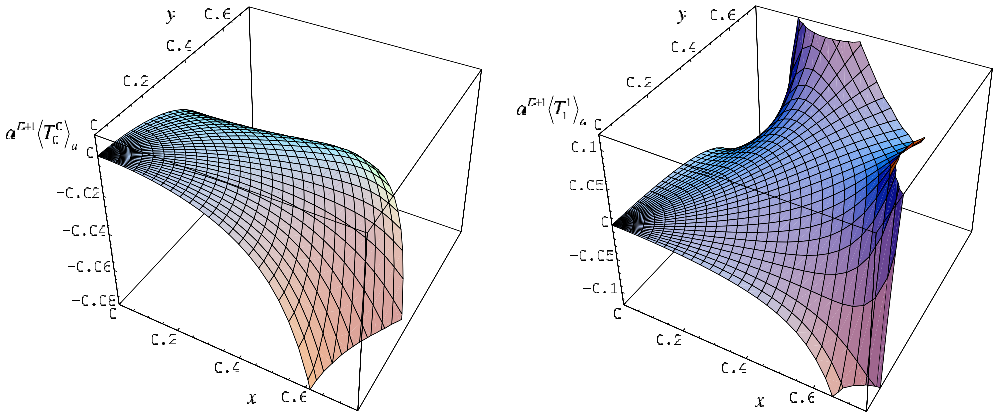

Figure 2. Dependence of the energy density and radial stress for a $D = 3$ conformally coupled scalar field, induced by a cylindrical boundary of radius a, on coordinates r and ϕ for the wedge with the opening angle $\phi_0 = \pi/2$. The variables on the axes are $x = (r/a)\cos\phi$ and $y = (r/a)\sin\phi$.

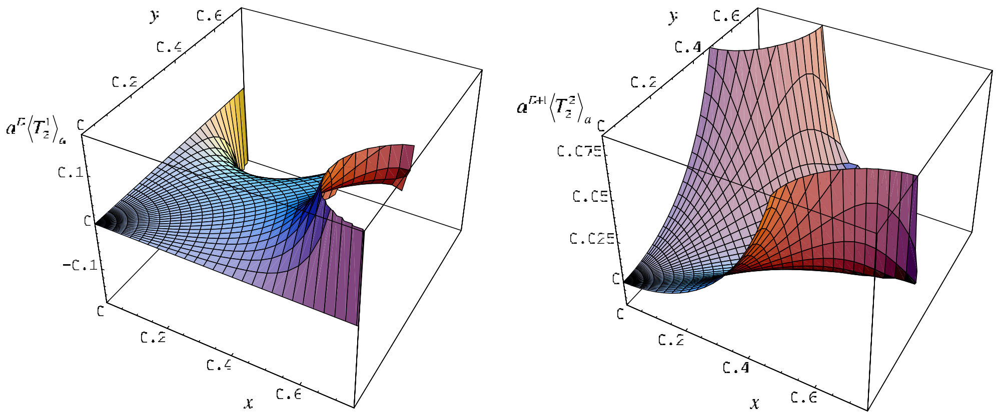

Figure 3. The same as in figure 2 for the off-diagonal $\frac{1}{2}$-component and the azimuthal stress.

5. Whightman function, the field square and the vacuum energy–momentum tensor in the region II

Now we turn to the region outside the cylindrical shell (region II in figure 1): $r > a, 0 \leqslant \phi \leqslant \phi_0$. The corresponding eigenfunctions satisfying boundary conditions (2.2) are obtained from (2.5) by the replacement

$$J_{qn}(\gamma r) \to g_{qn}(\gamma r, \gamma a) \equiv J_{qn}(\gamma r)Y_{qn}(\gamma a) - J_{qn}(\gamma a)Y_{qn}(\gamma r), \tag{5.1}$$

where $Y_{qn}(z)$ is the Neumann function. Now the spectrum for the quantum number γ is continuous. To determine the corresponding normalization coefficient β_α, we note that as the normalization integral diverges in the limit $\gamma = \gamma'$, the main contribution into the integral over radial coordinate comes from the large values of r when the Bessel functions can be replaced by their asymptotics for large arguments. The resulting integral is taken elementary and for the normalization coefficient in the region $r > a$ one finds

$$\beta_\alpha^2 = \frac{(2\pi)^{2-D}\gamma}{\phi_0\omega\left[J_{qn}^2(\gamma a) + Y_{qn}^2(\gamma a)\right]}. \tag{5.2}$$

Substituting the corresponding eigenfunctions into the mode sum formula (2.4), the positive frequency Whightman function is presented in the form

$$\langle 0|\varphi(x)\varphi(x')|0\rangle = \frac{1}{\phi_0}\int \frac{\mathrm{d}^N\mathbf{k}}{(2\pi)^N}\,\mathrm{e}^{\mathrm{i}\mathbf{k}(\mathbf{r}_\parallel-\mathbf{r}'_\parallel)}\sum_{n=1}^{\infty}\sin(qn\phi)\sin(qn\phi')$$
$$\times\int_0^\infty \mathrm{d}\gamma\,\frac{\gamma g_{qn}(\gamma r,\gamma a)g_{qn}(\gamma r',\gamma a)}{J_{qn}^2(\gamma a)+Y_{qn}^2(\gamma a)}\frac{\exp\left[\mathrm{i}(t'-t)\sqrt{\gamma^2+k^2}\right]}{\sqrt{\gamma^2+k^2}}. \tag{5.3}$$

To find the part in the Whightman function induced by the presence of the cylindrical shell, we subtract from (5.3) the corresponding function for the wedge without a cylindrical shell, given by (2.15). In order to evaluate the corresponding difference, we use the relation

$$\frac{g_{qn}(\gamma r,\gamma a)g_{qn}(\gamma r',\gamma a)}{J_{qn}^2(\gamma a)+Y_{qn}^2(\gamma a)} - J_{qn}(\gamma r)J_{qn}(\gamma r') = -\frac{1}{2}\sum_{s=1}^{2}\frac{J_{qn}(\gamma a)}{H_{qn}^{(s)}(\gamma a)}H_{qn}^{(s)}(\gamma r)H_{qn}^{(s)}(\gamma r'), \tag{5.4}$$

where $H_{qn}^{(s)}(z)$, $s = 1, 2$, are the Hankel functions. This allows us to present the Whightman function in the form (2.14) with the cylindrical shell induced part

$$\langle\varphi(x)\varphi(x')\rangle_a = -\frac{1}{2\phi_0}\int \frac{\mathrm{d}^N\mathbf{k}}{(2\pi)^N}\,\mathrm{e}^{\mathrm{i}\mathbf{k}(\mathbf{r}_\parallel-\mathbf{r}'_\parallel)}\sum_{n=1}^{\infty}\sin(qn\phi)\sin(qn\phi')$$
$$\times\sum_{s=1}^{2}\int_0^\infty \mathrm{d}\gamma\,\gamma\,\frac{J_{qn}(\gamma a)}{H_{qn}^{(s)}(\gamma a)}H_{qn}^{(s)}(\gamma r)H_{qn}^{(s)}(\gamma r')\frac{\exp\left[\mathrm{i}(t'-t)\sqrt{\gamma^2+k^2}\right]}{\sqrt{\gamma^2+k^2}}. \tag{5.5}$$

On the complex plane γ, we can rotate the integration contour on the right-hand side of this formula by the angle $\pi/2$ for $s = 1$ and by the angle $-\pi/2$ for $s = 2$. The integrals over the segments $(0, \mathrm{i}k)$ and $(0, -\mathrm{i}k)$ cancel out and after introducing the Bessel modified functions we obtain

$$\langle\varphi(x)\varphi(x')\rangle_a = -\frac{2}{\pi\phi_0}\int \frac{\mathrm{d}^N\mathbf{k}}{(2\pi)^N}\,\mathrm{e}^{\mathrm{i}\mathbf{k}(\mathbf{r}_\parallel-\mathbf{r}'_\parallel)}\int_k^\infty \mathrm{d}z\,\frac{z\cosh\left[(t-t')\sqrt{z^2-k^2}\right]}{\sqrt{z^2-k^2}}$$
$$\times\sum_{n=1}^{\infty}\sin(qn\phi)\sin(qn\phi')K_{qn}(zr)K_{qn}(zr')\frac{I_{qn}(za)}{K_{qn}(za)}. \tag{5.6}$$

Taking the coincidence limit for the arguments, from this formula we obtain the vacuum expectation value of the field square in the region $r > a$:

$$\langle\varphi^2\rangle_a = -\frac{2^{3-D}\pi^{\frac{1-D}{2}}}{\Gamma\left(\frac{D-1}{2}\right)a^{D-1}\phi_0}\sum_{n=1}^{\infty}\sin^2(qn\phi)\int_0^\infty \mathrm{d}z\,z^{D-2}\frac{I_{qn}(z)}{K_{qn}(z)}K_{qn}^2(zr/a). \tag{5.7}$$

Comparing with formulae (2.16) and (4.3), we see that the parts induced by the cylindrical shell in the regions I and II are obtained from each other by the interchange $I_{qn}(z) \leftrightarrows K_{qn}(z)$.

As for the region I, vacuum expectation value (5.7) diverges on the cylindrical surface. The leading term in the corresponding asymptotic expansion near this surface is obtained from that for the region I, formula (4.6), replacing $(a - r)$ by $(r - a)$. For large distances from the cylindrical surface, $r \gg a$, we introduce in (5.7) a new integration variable $y = zr/a$ and expand the integrand over a/r. The main contribution comes from the $n = 1$ term.

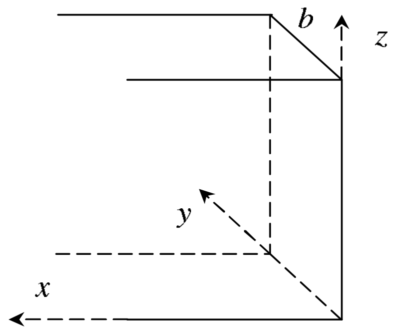

Figure 4. Geometry of two parallel plates with the interplate distance b perpendicularly intersected by the plate at $x = 0$.

By taking into account the value for the standard integral involving the square of the MacDonald function, to the leading order one finds

$$\langle\varphi^2\rangle_a \approx -\frac{\sin^2(q\phi)\Gamma\left(\frac{D-1}{2}+2q\right)\Gamma^2\left(\frac{D-1}{2}+q\right)}{\pi^{\frac{D+1}{2}}a^{D-1}\Gamma(D-1+2q)\Gamma^2(q)}\left(\frac{a}{r}\right)^{D-1+2q}. \tag{5.8}$$

For the part in the vacuum energy–momentum tensor induced by the cylindrical surface in the region $r > a$, from (2.3), (5.6) and (5.7) one has the following formulae:

$$\langle T_i^i\rangle_a = \frac{(4\pi)^{-\frac{D-1}{2}}}{\Gamma\left(\frac{D-1}{2}\right)a^{D+1}\phi_0}\sum_{n=1}^{\infty}\int_0^{\infty}\mathrm{d}z\, z^D\frac{I_{qn}(z)}{K_{qn}(z)} \times\left\{a_{i,qn}^{(+)}[K_{qn}(y)] - a_{i,qn}^{(-)}[K_{qn}(y)]\cos(2qn\phi)\right\}, \qquad y=\frac{zr}{a}, \tag{5.9}$$

$$\langle T_2^1\rangle_a = \frac{2(4\pi)^{-\frac{D-1}{2}}}{\Gamma\left(\frac{D-1}{2}\right)a^{D}\phi_0}\sum_{n=1}^{\infty}qn\sin(2qn\phi)\int_0^{\infty}\mathrm{d}z\, z^{D-1}\frac{I_{qn}(z)}{K_{qn}(z)} \times K_{qn}(y)\left[\frac{2\xi}{y}K_{qn}(y)+(1-4\xi)K'_{qn}(y)\right], \tag{5.10}$$

with the functions $a_{i,qn}^{(\pm)}[g(y)]$ defined by (4.10)–(4.12). By the way similar to that used above for the vacuum expectation value of the field square, it can be seen that for large distances from the cylindrical surface, $r \gg a$, the main contribution comes from the term with $n = 1$ and the components of the induced energy–momentum tensor behave as $\langle T_i^i\rangle_a \sim (a/r)^{D+1+2q}$, $\langle T_2^1\rangle_a \sim (a/r)^{D+2q}$. Near the cylindrical surface, the leading terms of the asymptotic expansions for the components of the energy–momentum tensor in the exterior region are obtained from the corresponding formulae for the interior region, formulae (4.23) and (4.25), replacing $(a-r)$ by $(r-a)$. As for the interior region, the vacuum forces acting on the wedge sides due to the presence of the cylindrical shell are attractive and the corresponding energy density is negative for both minimally and conformally coupled scalars.

6. Limiting case

In this section, we consider a limiting case of previous results, obtained in the limit $\phi_0 \to 0, r, a \to \infty$, assuming that $a - r$ and $a\phi_0 \equiv b$ are fixed. This limit corresponds to the geometry of two parallel plates separated by a distance b, perpendicularly intersected by the third plate (see figure 4). The vacuum expectation values of the energy–momentum tensor for this geometry of boundaries are investigated in [10] for special cases of minimally and conformally coupled massless scalar fields. Formulae presented below in this section generalize these results for the case of an arbitrary coupling and give an alternative representation of the vacuum energy–momentum tensor. We introduce rectangular coordinates $(x'^1, x'^2, \ldots, x'^D) = (x, y, z_1, \ldots, z_N)$ with the relations $x = a - r$, $y = r\phi$ in the limit under consideration. Below the components of the tensors in these coordinates we will denote by primes. In this limit, from the quantities corresponding to the wedge without a cylindrical surface we obtain the vacuum densities in the region between two parallel planes. These quantities are well investigated in the literature (see [27] for the case of general mixed boundary conditions) and below we will consider the additional part induced by the presence of the intersecting plate at $x = 0$. The corresponding vacuum expectation values are obtained from the expectation values $\langle\cdot\rangle_a$ investigated in the previous section. For this we note that in the limit under consideration one has $q = \pi/\phi_0 \to \infty$, and the order of the Bessel modified functions in formulae (4.3), (4.8) and (4.9) tends to infinity. Introducing a new integration variable $z \to qnz$, we can replace these functions by their uniform asymptotic expansions for large values of the order. The vacuum expectation value of the field square is presented in the form

$$\langle 0|\varphi^2|0\rangle = \langle\varphi^2\rangle^{(0)} + \langle\varphi^2\rangle^{(1)}, \tag{6.1}$$

where $\langle\varphi^2\rangle^{(0)}$ is the vacuum expectation value for two parallel planes, and

$$\langle\varphi^2\rangle^{(1)} = -\frac{x^{1-\frac{D}{2}}}{2^{D-2}\pi b^{\frac{D}{2}}}\sum_{n=1}^{\infty} n^{\frac{D}{2}-1}\sin^2(nv)K_{D/2-1}(nu) \tag{6.2}$$

is induced by the presence of the plate at $x = 0$. In (6.2), we use the notations

$$u = 2\pi x/b, \qquad v = \pi y/b. \tag{6.3}$$

Formula (6.2) can also be directly obtained by using the mode sum formula (2.4) with the eigenfunctions for the boundary geometry under consideration:

$$\varphi_\alpha = \frac{2\sin(k_1 x)}{\sqrt{(2\pi)^{D-1}b\omega}}\sin(\pi n y/b)\exp(\mathrm{i}\mathbf{k}\mathbf{r}_\parallel - \mathrm{i}\omega t), \tag{6.4}$$

where $0 < k_1 < \infty$, $n = 1, 2, \ldots$ and $\omega = \sqrt{k^2 + k_1^2 + (\pi n/b)^2}$.

The representation similar to (6.1) takes place for the components of the energy–momentum tensor:

$$\langle 0|T_k'^i|0\rangle = \left\langle T_k'^i\right\rangle^{(0)} + \left\langle T_k'^i\right\rangle^{(1)}, \tag{6.5}$$

where the expectation values $\left\langle T_k'^i\right\rangle^{(1)}$ are induced by the intersecting plate at $x = 0$. They are related to the quantities investigated in the previous section by formulae

$$\left\langle T_i'^i\right\rangle^{(1)} = \lim\left\langle T_i^i\right\rangle_a, \qquad \left\langle T_2'^1\right\rangle^{(1)} = -\lim\frac{1}{a}\left\langle T_2^1\right\rangle_a, \tag{6.6}$$

with lim corresponding to the limit $a \to \infty$, $\phi_0 \to 0$ for fixed $a - r$ and $a\phi_0$. Using the formulae for $\left\langle T_i^k\right\rangle_a$ for the induced quantities, one finds (no summation over i, $i = 0, 3, \ldots, D$)

$$\left\langle T_i'^i\right\rangle^{(1)} = \frac{\pi x^{1-\frac{D}{2}}}{2^{D-2}b^{\frac{D}{2}+2}}\sum_{n=1}^{\infty} n^{\frac{D}{2}+1}\left\{\frac{(4\xi-1)(D-1)}{nu}\sin^2(nv)K_{D/2}(nu) + \left[2\xi - \frac{1}{2} + \frac{\sin^2(nv)}{D-1}\right]K_{D/2-1}(nu)\right\}, \tag{6.7}$$

$$\langle T_1^{\prime 1}\rangle^{(1)} = \frac{\pi(4\xi-1)x^{1-\frac{D}{2}}}{2^{D-1}b^{\frac{D}{2}+2}}\sum_{n=1}^{\infty} n^{\frac{D}{2}+1}\cos(2nv)K_{D/2-1}(nu), \tag{6.8}$$

$$\langle T_2^{\prime 1}\rangle^{(1)} = \frac{\pi(4\xi-1)x^{1-\frac{D}{2}}}{2^{D-1}b^{\frac{D}{2}+2}}\sum_{n=1}^{\infty} n^{\frac{D}{2}+1}\sin(2nv)K_{D/2}(nu), \tag{6.9}$$

$$\langle T_2^{\prime 2}\rangle^{(1)} = \frac{\pi x^{1-\frac{D}{2}}}{2^{D-2}b^{\frac{D}{2}+2}}\sum_{n=1}^{\infty} n^{\frac{D}{2}+1}\left\{\frac{(4\xi-1)(D-1)}{nu}\sin^2(nv)K_{D/2}(nu) + \left[\frac{1}{2}+(4\xi-1)\sin^2(nv)\right]K_{D/2-1}(nu)\right\}, \tag{6.10}$$

with the notations from (6.3). Due to the presence of the MacDonald function in these formulae, the series are exponentially convergent. Note that in the alternative formulae for the energy–momentum tensor for minimally and conformally coupled scalar fields, given in [10], the convergence of the series is power law.

For $x > 0$, quantities (6.7)–(6.10) are finite on the plates $y = 0, b$:

$$\langle T_i^{\prime i}\rangle^{(1)}\big|_{y=0,b} = \frac{\pi x^{1-\frac{D}{2}}A_i}{2^{D-1}b^{\frac{D}{2}+2}}\sum_{n=1}^{\infty} n^{\frac{D}{2}+1}K_{D/2-1}(nu) \tag{6.11}$$

and $\langle T_2^{\prime 1}\rangle^{(1)}\big|_{y=0,b} = 0$. In particular, additional vacuum forces acting on the plates $y = 0, b$ due to the presence of the plate at $x = 0$ are determined by the component $\langle T_2^{\prime 2}\rangle^{(1)}$ and are attractive. For large distances from the plate $x = 0$, by using the asymptotic formula for the modified Bessel function, we can see that the main contribution comes from $n = 1$ term and to the leading order we find

$$\langle T_i^{\prime k}\rangle^{(1)} \sim u^{\frac{1-D}{2}}\,\mathrm{e}^{-u}, \qquad u \gg 1, \tag{6.12}$$

with u defined by relation (6.3). In this limit, the vacuum expectation values induced by the plate $x = 0$ are exponentially suppressed.

7. Conclusion

We have investigated the Whightman function, the vacuum expectation values of the field square and the energy–momentum tensor for a massless scalar field with a general curvature coupling parameter inside a wedge with a coaxial cylindrical boundary. We have assumed Dirichlet boundary conditions on the bounding surfaces. The generalization of the corresponding results for other boundary conditions is straightforward. The application of the generalized Abel-Plana summation formula for the series over the zeros of the Bessel function allowed us to extract from the expectation values the parts due to the wedge without a cylindrical boundary and to present the additional parts induced by this boundary in terms of exponentially convergent integrals. The vacuum densities for the geometry of a wedge without a cylindrical boundary are considered in section 3. We have derived formulae for the renormalized vacuum expectation values of the field square and the energy–momentum tensor, formulae (3.11), (3.17) and (3.18). These formulae can be further simplified for the important special case $D = 3$ (formulae (3.15), (3.25)–(3.28)). For a conformally coupled scalar, the energy–momentum tensor is diagonal and does not depend on the angular variable ϕ. The corresponding vacuum forces acting on the wedge sides are attractive for $\phi_0 < \pi$ and are repulsive for $\phi_0 > \pi$. The previous investigations of the problem are restricted to this case.

In section 4, we have investigated the additional expectation values for the field square and the energy–momentum tensor induced by the presence of the cylindrical surface. The field square is given by formula (4.3) and vanishes on the wedge sides $\phi = \phi_m$ for all points away from the cylindrical surface. The energy–momentum tensor induced by the cylindrical surface is non-diagonal and the corresponding components are determined by formulae (4.8) and (4.9). The off-diagonal component vanishes on the wedge sides. The additional vacuum forces acting on the wedge sides due to the presence of the cylindrical surface are determined by the $\frac{2}{2}$-component of the corresponding stress and are attractive for all values ϕ_0. On the wedge sides, the corresponding vacuum stresses in the directions parallel to the wedge sides are isotropic and the energy density is negative for both minimally and conformally coupled scalars. The vacuum expectation values diverge on the cylindrical surface. For the points with $|\phi - \phi_m| \gg 1 - r/a$, the leading divergences are the same as those for a cylindrical surface without the wedge. As an illustration of the general results, we have plotted in figures 2 and 3 the components of the vacuum energy–momentum tensor induced by the cylindrical surface in the case of a conformally coupled $D = 3$ scalar field for a wedge with the opening angle $\phi_0 = \pi/2$. The Whightman function, the vacuum expectation values of the field square and the energy–momentum tensor in the region outside the cylindrical shell are investigated in section 5. The formulae for these quantities differ from the corresponding formulae for the interior region by the interchange $I_{qn}(z) \leftrightarrows K_{qn}(z)$. For large distances from the cylindrical surface, $r \gg a$, the vacuum expectation values behave as $(a/r)^{D-1+2q}$ for the field square and as $(a/r)^{D+1+2q}$ for the diagonal components of the energy–momentum tensor. As in the case of interior region, the vacuum forces acting on the wedge sides due to the presence of the cylindrical shell are attractive. In section 6, we have considered a limiting case $\phi_0 \to 0, r, a \to \infty$, assuming that $a - r$ and $a\phi_0$ are fixed. This limit corresponds to the geometry of two parallel plates perpendicularly intersected by the third plate (see figure 4) and has been investigated previously in [10] for special cases of minimally and conformally coupled scalar fields. For general values of the curvature coupling parameter, the additional vacuum expectation values induced by the intersecting plate are given by formulae (6.2), (6.7)–(6.10). In particular, the corresponding energy–momentum tensor is diagonal on the parallel plates with the components (6.11) and the additional vacuum forces due to the presence of the intersecting plate are attractive. Vacuum densities induced by this plate are exponentially suppressed for large distances.

The generalization of the results obtained here for the Neumann or more general Robin boundary conditions is straightforward. For instance, for the Neumann case in the expressions (2.5) of the eigenfunctions, the function $\cos(qn\phi)$ stands instead of $\sin(qn\phi)$ and the quantum number n takes the values $0, 1, 2, \ldots$. In the case with a cylindrical boundary now the eigenvalues for γa are zeros for the derivative of the Bessel function. The formula to sum the series over these zeros can be taken from [16]. Now, in formulae (4.3), (4.8) and (4.9) for the vacuum expectation values, instead of the ratio $K_{qn}(z)/I_{qn}(z)$ the ratio of derivatives, $K'_{qn}(z)/I'_{qn}(z)$, will stand. Note that in this paper we have considered boundary induced vacuum densities which are finite away from the boundaries. As it has been mentioned in [28], the same results will be obtained in the model where instead of externally imposed boundary condition the fluctuating field is coupled to a smooth background potential that implements the boundary condition in a certain limit [29].

Acknowledgments

The work of AAS was supported by the ANSEF grant no 05-PS-hepth-89-70 and in part by the Armenian Ministry of Education and Science grant no 0124.

References

[1] Casimir H B G 1948 *Proc. K. Ned. Akad. Wet.* **51** 793
[2] Mostepanenko V M and Trunov N N 1997 *The Casimir Effect and Its Applications* (Oxford: Oxford University Press)
[3] Plunien G, Muller B and Greiner W 1986 *Phys. Rep.* **134** 87
[4] Bordag M, Mohidden U and Mostepanenko V M 2001 *Phys. Rep.* **353** 1
[5] Milton K A 2002 *The Casimir Effect: Physical Manifestation of Zero-Point Energy* (Singapore: World Scientific)
[6] Dowker J S and Kennedy G 1978 *J. Phys. A: Math. Gen.* **11** 895
[7] Deutsch D and Candelas P 1979 *Phys. Rev.* D **20** 3063
[8] Brevik I and Lygren M 1996 *Ann. Phys., NY* **251** 157
[9] Brevik I and Pettersen K 2001 *Ann. Phys., NY* **291** 267
[10] Actor A A and Bender I 1996 *Fortschr. Phys.* **44** 281
[11] Nesterenko V V, Lambiase G and Scarpetta G 2001 *J. Math. Phys.* **42** 1974
[12] Rezaeian A H and Saharian A A 2002 *Class. Quantum Grav.* **19** 3625
[13] Apps J S and Dowker J S 1998 *Class. Quantum Grav.* **15** 1121
[14] Dowker J S 2000 Divergences in the Casimir energy *Preprint* hep-th/0006138
[15] Nesterenko V V, Pirozhenko I G and Dittrich J 2003 *Class. Quantum Grav.* **20** 431
[16] Saharian A A 1987 *Izv. Akad. Nauk Arm. SSR Mat.* **22** 166
Saharian A A 1987 *Sov. J. Contemp. Math. Anal.* **22** 70 (Engl. Transl.)
Saharian A A 2000 The generalized Abel-Plana formula. Applications to Bessel functions and Casimir effect *Preprint* hep-th/0002239
[17] Birrell N D and Davies P C W 1982 *Quantum Fields in Curved Space* (Cambridge: Cambridge University Press)
[18] Grigoryan L Sh and Saharian A A 1986 *Dokl. Akad. Nauk Arm. SSR* **83** 28 (in Russian)
Grigoryan L Sh and Saharian A A 1987 *Izv. Akad. Nauk Arm. SSR Fiz.* **22** 3
Grigoryan L Sh and Saharian A A 1987 *Sov. J. Contemp. Phys.* **22** 1 (Engl. Transl.)
Saharian A A 2001 *Phys. Rev.* D **63** 125007
Saharian A A and Setare M R 2003 *Class. Quantum Grav.* **20** 3765
Saharian A A and Setare M R 2004 *Int. J. Mod. Phys.* A **19** 4301
Saharian A A and Bezerra de Mello E R 2004 *J. Phys. A: Math. Gen.* **37** 3543
[19] Saharian A A 1988 *Izv. Akad. Nauk Arm. SSR Fiz.* **23** 130
Saharian A A 1988 *Sov. J. Contemp. Phys.* **23** 14 (Engl. Transl.)
[20] Romeo A and Saharian A A 2001 *Phys. Rev.* D **63** 105019
[21] Saharian A A 2005 *Nucl. Phys.* B **712** 196
Saharian A A 2004 *Phys. Rev.* D **70** 064026
[22] Abramowitz M and Stegun I A 1964 *Handbook of Mathematical Functions* (Washington, DC: National Bureau of Standards)
[23] Prudnikov A P, Brychkov Yu A and Marichev O I 1986 *Integrals and Series: Special Functions* vol 2 (Newark, NJ: Harwood Academic)
[24] Kennedy G, Critchley R and Dowker J S 1980 *Ann. Phys., NY* **125** 346
[25] Candelas P 1982 *Ann. Phys., NY* **143** 241
[26] Ford L H and Svaiter N F 1998 *Phys. Rev.* D **58** 065007
[27] Romeo A and Saharian A A 2002 *J. Phys. A: Math. Gen.* **35** 1297
[28] Graham N, Jaffe R L, Khemani V, Quandt M, Scandurra M and Weigel H 2003 *Phys. Lett.* B **572** 196
[29] Graham N, Jaffe R L, Khemani V, Quandt M, Scandurra M and Weigel H 2002 *Nucl. Phys.* B **645** 49
Graham N, Jaffe R L and Weigel H 2002 *Int. J. Mod. Phys.* A **17** 846